Tracer Diffusion of ^{63}Ni in Fe-17 wt pct Cr-12 wt pct Ni

R. A. PERKINS

The tracer diffusion of ^{63}Ni in Fe-17 Cr-12 Ni by both volume and grain boundary transport has been studied from 600° to 1250°C. The use of an RF sputtering technique for serial sectioning allowed the determination of very small volume diffusion coefficients at the lower temperatures. Volume diffusion of nickel in this alloy was observed to be much slower than in pure iron or austenitic stainless steel at comparable temperatures. The volume diffusion coefficient is described by $D_V = 8.8 \exp(-60{,}000/RT)$ cm^2/s and grain boundary diffusion is described by $\delta D_{gb} = 3.7 \times 10^{-9} \exp(-32{,}000/RT)$ cm^3/s.

SEVERAL investigations[1-9] have been reported which describe the diffusion parameters of Fe, Cr, and Ni transport in pure iron and various stainless steels by both volume and grain boundary diffusion mechanisms. Results from previous studies[1-4] on nickel diffusion are summarized in Tables I and II where the parameters pertain to the usual Arrhenius-type equation relating the diffusion coefficient to temperature, $D = D_0 \exp[Q/RT]$. In an attempt to obtain some basic information about diffusion in Fe-Cr-Ni alloys, the volume and grain-boundary self-diffusion of ^{63}Ni in the ternary alloy Fe-17 wt pct Cr-12 wt pct Ni have been investigated as part of an overall study to examine self-diffusion for all three constituents. This alloy and 316 stainless steel are of similar composition; therefore, in addition to the basic interest in diffusion in fcc iron-based alloys, the study will help characterize diffusion in 316 stainless steel.

Table I. Volume Diffusion of Nickel

Solvent	Frequency Factor, cm^2/s	Activation Energy kcal/mole	Reference
	D_v^0	Q_v	
Fe	0.77	67.0	1
Fe	1.25	67.7	2
Fe-9 pct Ni Steel	5.6×10^{-5}	46.7	3
Fe-17 Cr-12 Ni	8.8×10^{-3}	60.0	this study
Fe-20 Cr-25 Ni/Nb steel	4.06	67.5	4

Table II. Grain Boundary Diffusion of Nickel

Solvent	Frequency Factor, cm^3/s	Activation Energy kcal/mole	Reference
	δD_{gb}^0	Q_{gb}	
Fe	2.5×10^{-6}	44.5	2
Fe-9 pct Ni steel	1.8×10^{-9}	28.6	3
Fe-17 Cr-12 Ni	3.7×10^{-9}	31.5	this study
Fe-20 Cr-25 Ni/Nb steel	1.5×10^{-7}	47.9	4

R. A. PERKINS, formerly Presidential Intern, Metals and Ceramics Division, Oak Ridge National Laboratory, Oak Ridge, Tenn. 37830, is now with Globe-Union Inc., Milwaukee, Wisc. 53201.

Manuscript submitted December 4, 1972.

The data are of value in determining the effects of major and possibly minor constituents upon the atomic motion of nickel in various austenitic steels. A method has been used which allows the determination of true volume self-diffusion coefficients down to 600°C; whereas, most investigations yield an upward deviation from the Arrhenius plot at low temperatures due to "enhanced diffusion." These low temperatures are in the range of many practical engineering applications and will aid in relating basic transport phenomena to practical problems.

EXPERIMENTAL PROCEDURE

The Fe-17 wt pct Cr-12 wt pct Ni alloy was prepared from high-purity Fe, Cr, and Ni by arc melting under an argon atmosphere. The alloy button was inverted and remelted several times to obtain an even distribution of the constituents and swaged into a rod 1.27 cm in diameter. The swaged rod was cut into pieces 7 cm in length which were wrapped in tantalum foil and preannealed at 1300°C for 96 h in a high-purity argon atmosphere. The composition of the alloy is given in Table III. Specimens from the rod were analyzed at three points along its length to check the homogeneity of the alloy. The grain size was determined to be approximately ASTM No. 0, or 8 grains/mm^2. Cylindrical specimens 1.2 cm in diam and 0.3 cm in length were then cut from the alloy rods. One face of each specimen was polished through 4/0 emery paper. Those specimens used for the low temperature anneals (600° to 750°C) were further polished through 0.05 μ alumina powder and alternately etched and polished three times to remove strained material. (A specimen prepared each way was run at 1000°C, and no difference was observed in either the diffusion coefficient obtained or the resolution of the volume diffusion zone near the surface.) The ^{63}Ni isotope was then evaporated onto the specimen from a tungsten filament under vacuum or deposited dropwise onto the specimen with subsequent evaporation of the solution. The former technique was used exclusively for specimens run at tempera-

Table III. Composition, wt pct, of Alloy

Fe	Cr	Ni	Si	Mn	Al	Nb	Ta	C
70.45	16.75	12.05	0.1	0.003	<0.02	<0.03	<0.05	0.0058

tures below 1100°C. Specimens were then wrapped in tantalum foil and encapsulated in quartz ampoules along with zirconium turnings to reduce the oxygen pressure during the diffusion anneal. Each ampoule was sealed with the appropriate argon pressure to create a pressure of ~1 atm inside the ampoule at the diffusion anneal temperature. Diffusion anneals were run at approximately 50°C intervals from 600° to 1250°C with the temperature controlled to ± 2°C. Details of the anneals are listed in Table IV.

Sectioning to analyze the volume diffusion zone at small penetration values was accomplished by a radio-frequency sputtering technique to be described fully in a later paper.[10] Basically, a portion of the specimen face was exposed to argon ion bombardment and a fraction of the material removed from the surface was collected on planchets under the specimen. A rim about 1 mm wide around the circumference of the specimen face was shielded so surface diffusion down the side of the specimen did not influence the results. The section thickness was determined by weighing the specimen before and after the sputtering process and dividing the loss into increments, the size of the increments being determined by the length of time material was deposited on each planchet. The activity of ^{63}Ni in the material deposited on the planchets was measured using a partially depleted surface barrier detector. For comparative purposes the volume diffusion coefficients were determined by a conventional grinding technique at two temperatures—1100° and 1250°C.

After the volume diffusion zone was sectioned, the specimen diameter was reduced to remove the effects of any surface diffusion of ^{63}Ni down the sides of the specimen during the anneal. The concentration profile in the grain boundary diffusion zone was then measured by a surface decrease counting technique in which the activity of the surface was measured after removing successive layers. Because ^{63}Ni emits only low-energy (0.063 MeV) β-radiation, the radiation is very strongly absorbed in the alloy, and the activity at the surface is characteristic of only a very thin layer of the specimen. From Gruzin's method,[12] if the radiation is strongly absorbed, the profile obtained from counting the decrease in the surface activity is completely analogous to that obtained from the residual activity counting technique. This technique was used previously for ^{63}Ni diffusion in Cu,[11] Ni,[12] and Fe.[1]

Table IV. Volume and Grain Boundary Diffusion Coefficients for Nickel in Fe-17Cr-12Ni

Temp., °C	Time, s	Volume Diffusion Zone Width, 10^{-4} cm	D_v, cm^2/s	δD_{gb}, cm^3/s
1253	1.152×10^5	51.6*	4.078×10^{-11}	
1250	1.082×10^4	7.5†	2.607×10^{-11}	1.091×10^{-13}
1248	1.152×10^5	48.1*	5.433×10^{-11}	7.822×10^{-14}
1200	1.224×10^4	5.3†	1.344×10^{-11}	6.422×10^{-14}
1149	1.476×10^4	5.4†	4.166×10^{-12}	7.004×10^{-14}
1099	5.184×10^5	35.0*	4.659×10^{-12}	2.412×10^{-14}
1098	2.886×10^4	5.7†	1.216×10^{-12}	5.186×10^{-14}
1051	1.782×10^5	4.4†	1.350×10^{-12}	1.908×10^{-14}
1002	2.376×10^5	3.6†	4.403×10^{-13}	2.183×10^{-14}
1000	3.456×10^5	6.1†	3.333×10^{-13}	2.624×10^{-14}
949	4.392×10^5	7.6†	2.240×10^{-13}	8.436×10^{-15}
898	5.184×10^5	4.0†	9.619×10^{-14}	4.477×10^{-15}
851	1.728×10^6	4.6†	1.049×10^{-14}	2.588×10^{-15}
799	1.8144×10^6	4.6†	7.984×10^{-15}	7.688×10^{-16}
748	2.8512×10^6	1.7†	8.950×10^{-16}	6.510×10^{-16}
702	4.0716×10^6	0.87†	5.725×10^{-16}	4.430×10^{-16}
650	3.9744×10^6	0.46†	4.747×10^{-17}	1.401×10^{-16}
603	5.0112×10^6	0.22†	7.081×10^{-18}	4.416×10^{-17}

*Sectioned by hand grinding.
†Sectioned by rf sputtering.

DATA ANALYSIS

In the region of the specimen where volume diffusion predominates, the tracer diffusion is described by the "thin film" solution to Fick's Second Law for a semi-infinite medium

$$A(x, t) = \frac{M}{\sqrt{\pi Dt}} \exp\left(-\frac{x^2}{4Dt}\right) \quad [1]$$

where $A(x, t)$ is the activity at a distance x into the specimen at time t, M is the initial total activity per unit area in the isotope layer and D is the volume diffusion coefficient. Therefore, $\ln A$ plotted vs x^2 should yield a straight line with the slope equal to $-1/(4Dt)$. This straight line relation was observed near the surface for all specimens; however, the activity deviated from the linear plot at distances greater than approximately $2(Dt)^{1/2}$ as various short-circuiting effects became important. Far from the surface and the volume diffusion region, grain boundary diffusion predominates. The grain-boundary diffusion equation has been solved for a grain boundary perpendicular to the surface of a semiinfinite medium for: 1) a constant surface concentration,[12,14] and 2) an instantaneous surface concentration.[16] Le Claire[15] and Suzuoka[16] have shown that the grain-boundary diffusion coefficients obtained experimentally from serial sectioning are essentially the same for both boundary conditions when analyzed according to either Whipple's solution or Suzuoka's solution. Fisher's solution yields a value of $\frac{1}{2}$ to $\frac{1}{3}$ the value obtained from the other two solutions. Whipple's solution for grain boundary self-diffusion can be written in the form[9]

$$\delta D_{gb} = \left(\frac{\partial \ln A}{\partial x^{6/5}}\right)^{-5/3} \left(\frac{4D_v}{t}\right)^{1/2} \left(\frac{\partial \ln A}{\partial (\eta\beta^{-1/2})^{6/5}}\right)^{5/3} \quad [2]$$

where D_{gb} is the grain boundary diffusion coefficient, δ is the grain boundary width, η is the dimensionless distance parameter $x/(Dt)^{1/2}$, and β is the ratio of D_{gb} and D_v in the form: $\beta = (D_{gb}/D_v - 1)\delta/2(Dt)^{1/2}$. To apply this solution to multicomponent systems, δD_{gb} must be replaced by $\alpha\delta D_{gb}$[17] where α is the equilibrium ratio of the grain-boundary tracer concentration to the lattice concentration and allows for the grain boundary segregation of the diffusing species. From a consideration of the similar ionic radii of Ni, Fe, and Cr, α is assumed to be unity for each constituent in the present system.[18] For grain boundary diffusion, the logarithm of the activity plotted vs $x^{6/5}$ should yield the best straight line fit.[19,20] Furthermore, from numerical analysis LeClaire[15] has shown that the slope of $\ln A$ vs $(\eta\beta^{-1/2})^{6/5}$ is nearly independent of $\eta\beta^{-1/2}$ such that $(\partial \ln A/\partial(\eta\beta^{-1/2})^{6/5})$ is approximately 0.74 over the penetration range commonly used experimentally. The value of $\partial \ln A/\partial(\eta\beta^{-1/2})^{6/5}$ is also essentially independent of β when $\beta > 10$. Such was observed in the present work for those specimens annealed at 1150°C and

lower. Therefore, the grain boundary diffusion coefficient was calculated from a linear least squares fit of the data plotted as ln A vs $x^{6/5}$ at large distances into the specimen using Eq. [2].

RESULTS AND DISCUSSION

The concentration profile obtained for the specimen annealed at 603°C is plotted as the logarithm of the activity vs x^2 in Fig. 1. The volume diffusion zone is contained within the first 0.22 μ from the surface, and the grain boundary diffusion zone extends from 30 μ inward. Because different sectioning and counting techniques were used to analyze the two zones, the activity from the two sets of data were related empirically to yield the complete curve. The volume diffusion zone is plotted on an expanded x^2 scale in Fig. 2 yielding the straight line relationship expected from the "thin film" solution of Fick's Second Law. The grain boundary diffusion zone is plotted as ln A vs $x^{6/5}$ in Fig. 3 indicating the type of linear plot from which δD_{gb} is calculated.

Table III contains the volume and grain boundary diffusion coefficients measured experimentally in this research. Included in the table is the width of the volume diffusion zone which exhibited a typical Gaussian relation between the activity of ^{63}Ni and the penetration distance squared. Therefore very fine sectioning techniques were required to analyze this zone and obtain a true volume diffusion coefficient below 800°C instead of observing "enhanced diffusion"[18] due to short circuiting mechanisms. The sputtering technique which had been developed provided a method of removing very thin sections easily and rapidly. As indicated in Table IV, at 1100° and 1250°C specimens were annealed for a short time and sectioned by sputtering, and also specimens were annealed for a long time and sectioned by grinding in order to determine the correlation of the results of the sputtering technique with the results of more conventional sectioning techniques. The diffusion coefficient obtained from grinding is approximately a factor of two higher than that obtained from sputtering. This slight difference is to be expected since the diffusion zone necessary for grinding is much wider, and therefore, short-circuiting effects will contribute to a greater degree to the region attributed to volume diffusion.

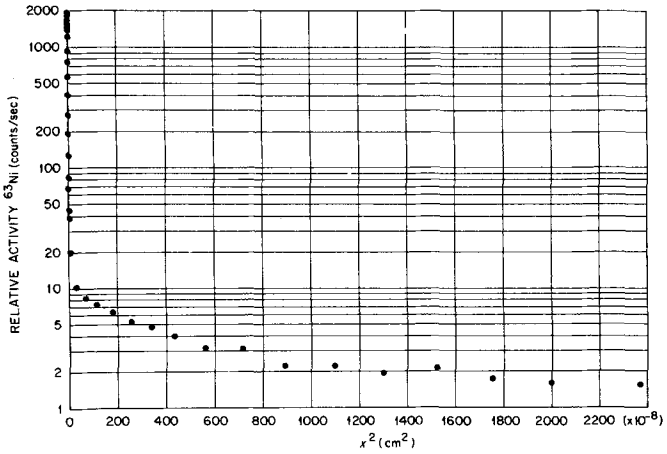

Fig. 1—Diffusion of ^{63}Ni in Fe-17 Cr-12 Ni at 603°C for 5.0112×10^6 s.

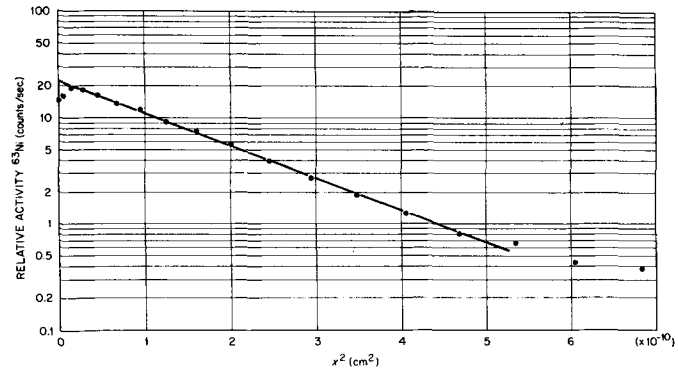

Fig. 2—Volume diffusion of ^{63}Ni in Fe-17 Cr-12 Ni at 603°C for 5.0112×10^6 s.

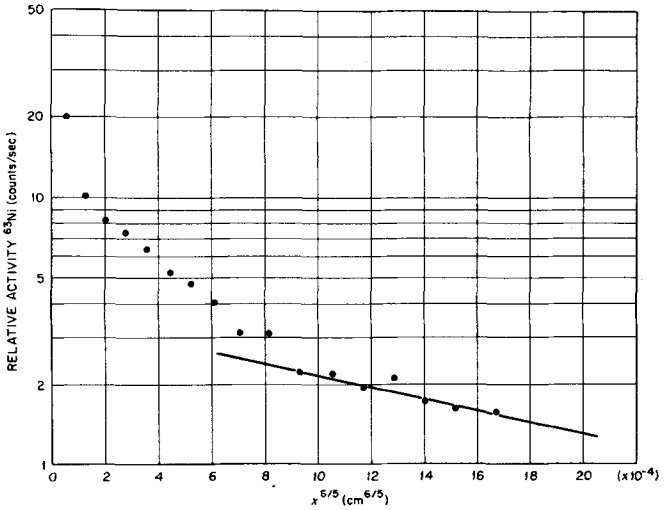

Fig. 3—Grain-boundary diffusion of ^{63}Ni in Fe-17 Cr-12 Ni at 603°C for 5.0112×10^6 s.

The results of the volume diffusion analysis listed in Table III are shown on an Arrhenius plot in Fig. 4. The results from the specimens sectioned by grinding are shown in Fig. 4 but were not included in the least squares fit from which the diffusion parameters were calculated. Obviously, there is no evidence of "enhanced diffusion" resulting from the contribution of short-circuiting mechanisms down to 600°C. The temperature dependence of the volume diffusion is:

$$D_v = (8.8 \pm 1.7) \times 10^{-3} \exp\left[-(60{,}000 \pm 2600)/RT\right] \text{ cm}^2/\text{s} \quad [3]$$

The error limits indicate a ninety percent confidence in the calculated values using standard Student t statistics.

In Fig. 4 the results of the present investigation are compared to nickel volume diffusion in pure iron and two alloys. Nickel diffusion in the present alloy is appreciably slower than in pure iron or Fe-20 Cr-25 Ni/Nb steel, but is about the same as in a 9 pct Ni steel. In nickel steels, D_v° and Q_v for nickel volume self-diffusion have been observed to decrease with increasing nickel content from 2.5 to 9 pct Ni.[4] In several austenitic stainless steels, D_v° has been observed

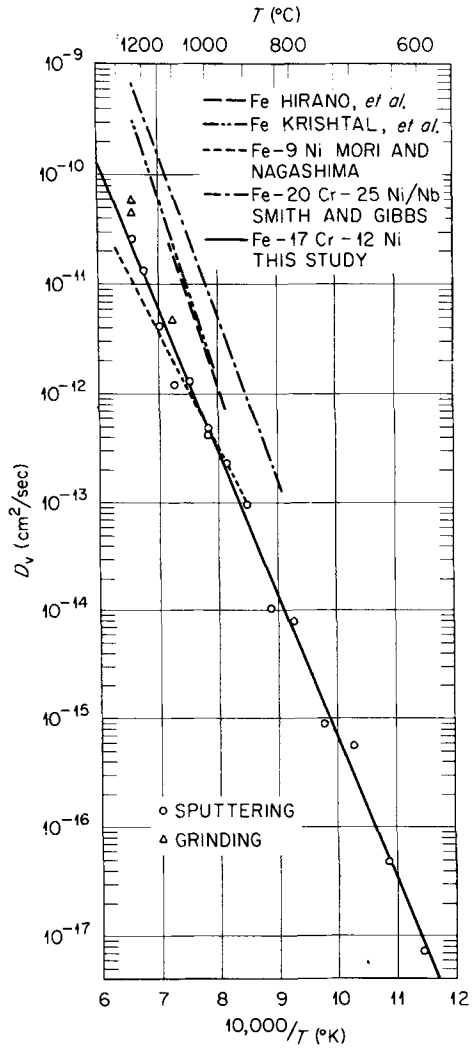

Fig. 4—Volume diffusion of ^{63}Ni.

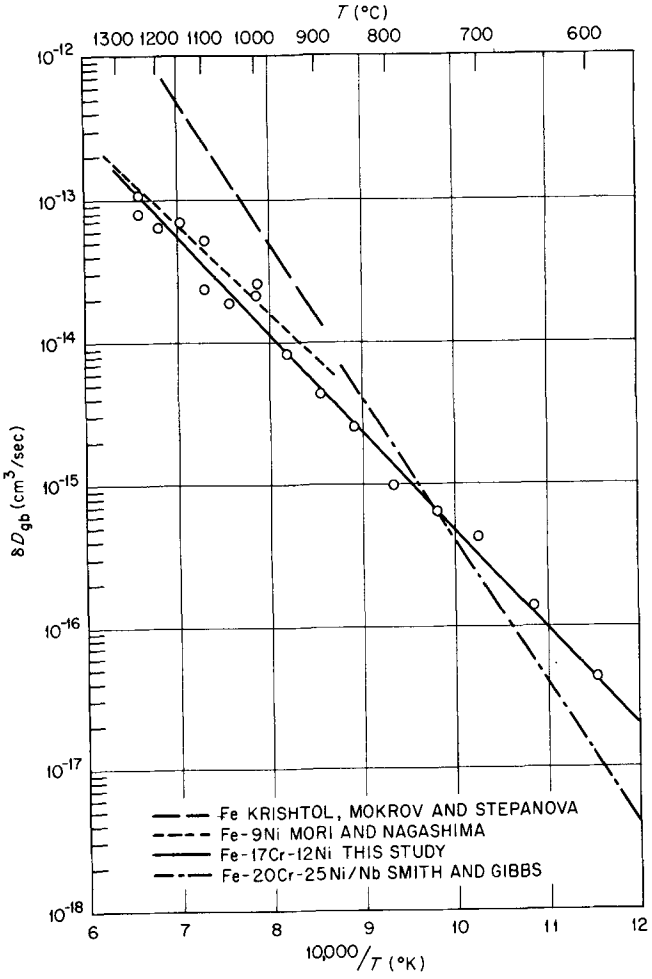

Fig. 5—Grain-boundary diffusion of ^{63}Ni.

to increase while Q_v decreased with increasing nickel content for chromium volume self-diffusion.[21] Studies of the effect of nickel content upon the volume self diffusion of iron in Fe-Ni alloys have been made, indicating that although varying trends on D_v° were observed, Q_v always decreased with increasing nickel content.[22] For iron volume diffusion in austenite, chromium additions have been observed to increase D_v° and Q_v.[22,23] These observations have led to the conclusions that the atomic bond strength in the austenitic lattice decreases as the nickel content increases[2] and increases as the chromium content increases.[22] The variation in Q_v for the alloys listed in Table I is opposite the trend expected based upon the nickel content. The Q_v decreases for the 9 pct Ni steel but for the other alloys the chromium effect predominates as Q_v increases with (Cr + Ni) content. The frequency factor, D_0, also increases rapidly with (Cr + Ni) content; an increase to which both elements may be contributing. Due to the gross differences in concentration between the alloys, the effects of minor constituents cannot be estimated.

The Arrhenius plot for the grain boundary diffusion coefficients listed in Table III is shown in Fig. 5. In order to calculate δD_{gb} from Eq. [2], the value of D_v at a particular temperature was calculated from Eq. [3] to use in Eq. [2]. The temperature dependence of δD_{gb} is given by

$$\delta D_{gb} = (3.7 \pm 0.5) \times 10^{-9} \exp[-(32{,}000 \pm 1900)/RT]\,\text{cm}^3/\text{s} \quad [4]$$

The values obtained for δD_{gb} compare well with the results obtained for nickel diffusion in the nickel and stainless steels previously mentioned as shown in Fig. 5. However, the diffusion parameters, δD_{gb}° and Q_{gb} which are compared in Table I, vary greatly. Smith and Gibbs[3] used the Whipple analysis for the Fe-20 Cr-25 Ni/Nb steel and Mori and Nagashima[4] used the Suzuoka analysis for the 9 pct Ni steel but this would not cause differences of the magnitude observed when comparing the results. The activation energy and frequency factor increase with increasing (Ni + Cr) content; the same trend observed for volume diffusion. The nickel content had been previously observed to have no consistent effect upon δD_{gb}° and Q_{gb} for grain-boundary diffusion in nickel steels of 2.5 to 9 pct Ni.[4] The grain boundary diffusion coefficients in the three alloys are of the same general magnitude while the results for pure iron are much higher. If the results of the two steels were expanded over a wider temperature range, larger differences in the diffusion coefficients might appear since the results for pure iron coincide well with an extrapolation of results of Smith and Gibbs. Therefore, this

indicates that the differences are not necessarily due to the narrower temperature ranges of the previous studies.

Because both volume and grain boundary diffusion measurements were obtained from each specimen, the interrelation between the two processes must be considered to determine what degree of error is inherent in the results. Suzuoka[16] has derived a grain boundary parameter $n = b/(Dt)^{1/2}$ where, assuming cubic grains, b is one half the length of an edge of a grain. Then from a knowledge of n and β for a particular specimen, the error in D_v caused by the grain boundary diffusion can be estimated.* The error was determined to range from approximately +4 pct for the 1250°C specimen to essentially 0 for the 600°C specimen. Suzuoka[19] has also determined an "observable range" from which δD_{gb} can be calculated such that the volume diffusion from the surface contributes less than 1 pct to the activity measured from serial sectioning. The minimum of the "observable range" varied from approximately 33 μ for the 1250°C specimen to less than 0.4 μ for the 600°C specimen. As can be seen in Fig. 1, the portion of the concentration profile attributed to grain boundary diffusion is well beyond the minimum limit of the "observable range." This indicates a large intermediate range which results from a combination of volume diffusion, grain boundary diffusion and diffusion along high-diffusivity dislocation pipes. The limit of the observable range is dependent upon the ratio of δD_{gb} to D_v. At low temperatures "enhanced diffusion" along dislocation pipes becomes predominant over volume diffusion, and only if very fine sectioning techniques are used can the volume diffusion be observed. In an analogous manner, to avoid the contributions of "enhanced diffusion" down dislocation pipes to the grain boundary diffusion range, the minimum limit would be dependent upon the ratio of δD_{gb} to D_{enhanced} which is much smaller than δD_{gb} to D_v. Therefore, the minimum limit would be much larger to avoid contributions from enhanced diffusion to the grain boundary region. As the temperature of the diffusion anneal increased, the grain boundary diffusion range more nearly approached the minimum limit calculated from D_v. Finally, Suzuoka[15] has indicated that as the grain size increases the assumption concerning the concentration at the edges of the grain boundary slab is better fulfilled. In accord with this effect, the apparent D_{gb} has been observed to decrease with grain size[16,24] or as the range of penetration increases relative to the grain size. To avoid this effect, the grain size should be much greater than the range of penetration. This situation was not maintained in the present study nor in the other alloys to which reference has been made. However, for the diffusion in pure iron the ratio of grain size to penetration distance was much larger and could partially account for the much higher results which were obtained.

*Fig. 9, Ref. 16.

CONCLUSIONS

1) The radiofrequency sputtering technique has been observed to be a useful and reliable method of serial sectioning specimens with very shallow volume diffusion zones.

2) The volume and grain boundary diffusion coefficients of ^{63}Ni in Fe-17 Cr-12 Ni have been determined from 600° to 1250°C and are represented by Eqs. [3] and [4], respectively.

3) The activation energies and frequency factors of volume and grain boundary diffusion of ^{63}Ni are observed to drop from pure iron to 9 pct Ni steel and then increase with (Cr + Ni) content in three austenitic iron alloys.

4) The rate of volume diffusion of nickel varies greatly for the three iron alloys discussed while the rate of grain boundary diffusion of nickel varies very little with alloy composition.

REFERENCES

1. K. Hirano, N. Cohen, and B. L. Averbach: *Acta Met.*, 1961, vol. 9, pp. 440-45.
2. M. A. Krishtal, A. P. Mokrov, and O. V. Stepanova: *Fiz. Metal. Metalloved*, 1967, vol. 24, pp. 688-92.
3. A. F. Smith and G. B. Gibbs: *Metals Sci. J.*, 1969, vol. 3, pp. 93-94.
4. N. Mori and S. Nagashima: *Nippon Kinzoku Gakkaishi*, 1966, vol. 30, pp. 455-60.
5. C. Stawström and M. Hillert: *J. Iron Steel Inst.*, 1969, vol. 207, pp. 77-85.
6. A. W. Bowen and G. M. Leak: *Met. Trans.*, 1970, vol. 1, pp. 1695-1700.
7. B. Sparke, D. W. James, and G. M. Leak: *J. Iron Steel Inst.*, 1965, vol. 203, pp. 152-53.
8. V. Linnenbom, M. Tetenbaum, and C. Cheek: *J. Appl. Phys.*, 1955, vol. 26, pp. 932-36.
9. P. Lacombe, P. Guiraldenq, and C. Leymonie: *Radioisotopes in the Physical Sciences and Industry*, pp. 179-92, 1962.
10. R. A. Perkins, R. A. Padgett, Jr., and N. K. Tunali: Oak Ridge National Laboratory, Oak Ridge, Tennessee, accepted for publication in *Met. Trans.*
11. C. A. Mackliet: *Phys. Rev.*, 1958, vol. 109, pp. 1964-70.
12. R. E. Hoffman, F. W. Pikus, and R. A. Ward: *AIME Trans.*, 1956, vol. 206, pp. 483-86.
13. J. C. Fisher: *J. Appl. Phys.*, 1951, vol. 22, pp. 74-77.
14. R. T. P. Whipple: *Phil. Mag.*, 1954, vol. 45, pp. 1225-36.
15. A. D. LeClaire: *Brit. J. Appl. Phys.*, 1963, vol. 14, pp. 351-56.
16. T. Suzuoka: *J. Phys. Soc. Japan*, 1964, vol. 19, pp. 839-51.
17. G. B. Gibbs: *Phys. Status Solidi*, 1966, vol. 16, pp. K27-K29.
18. A. F. Smith and G. B. Gibbs: *Metals Sci. J.*, 1968, vol. 2, pp. 47-50.
19. T. Suzuoka: *Japan Inst. Metals*, 1961, vol. 2, pp. 25-33.
20. H. S. Levine and C. J. MacCallum: *J. Appl. Phys.*, 1960, vol. 31, pp. 595-99.
21. I. E. Sulayev, A. N. Kurasov, N. A. Karpov, and A. V. Rabinovich: *Russian Met.*, 1970, vol. 4, pp. 150-53.
22. M. A. Krishtal: *Diffusion Processes in Iron Alloys*, A. Wald, trans., J. J. Becken, ed., p. 140, Israel Program for Scientific Translations, Ltd., 1970.
23. C. Leymonie: *Radioactive Tracers in Physical Metallurgy*, V. Griffiths, trans., p. 74, London, Chapman and Hall, 1963.
24. R. E. Hoffman and D. Turnbull: *J. Appl. Phys.*, 1951, vol. 22, pp. 634-39.